

NASA/TM-2008-215306



Plan for the Characterization of HIRF Effects on a Fault-Tolerant Computer Communication System

*Wilfredo Torres-Pomales, Mahyar R. Malekpour, Paul S. Miner, and Sandra V. Koppen
Langley Research Center, Hampton, Virginia*

May 2008

The NASA STI Program Office . . . in Profile

Since its founding, NASA has been dedicated to the advancement of aeronautics and space science. The NASA Scientific and Technical Information (STI) Program Office plays a key part in helping NASA maintain this important role.

The NASA STI Program Office is operated by Langley Research Center, the lead center for NASA's scientific and technical information. The NASA STI Program Office provides access to the NASA STI Database, the largest collection of aeronautical and space science STI in the world. The Program Office is also NASA's institutional mechanism for disseminating the results of its research and development activities. These results are published by NASA in the NASA STI Report Series, which includes the following report types:

- **TECHNICAL PUBLICATION.** Reports of completed research or a major significant phase of research that present the results of NASA programs and include extensive data or theoretical analysis. Includes compilations of significant scientific and technical data and information deemed to be of continuing reference value. NASA counterpart of peer-reviewed formal professional papers, but having less stringent limitations on manuscript length and extent of graphic presentations.
- **TECHNICAL MEMORANDUM.** Scientific and technical findings that are preliminary or of specialized interest, e.g., quick release reports, working papers, and bibliographies that contain minimal annotation. Does not contain extensive analysis.
- **CONTRACTOR REPORT.** Scientific and technical findings by NASA-sponsored contractors and grantees.

- **CONFERENCE PUBLICATION.** Collected papers from scientific and technical conferences, symposia, seminars, or other meetings sponsored or co-sponsored by NASA.
- **SPECIAL PUBLICATION.** Scientific, technical, or historical information from NASA programs, projects, and missions, often concerned with subjects having substantial public interest.
- **TECHNICAL TRANSLATION.** English-language translations of foreign scientific and technical material pertinent to NASA's mission.

Specialized services that complement the STI Program Office's diverse offerings include creating custom thesauri, building customized databases, organizing and publishing research results ... even providing videos.

For more information about the NASA STI Program Office, see the following:

- Access the NASA STI Program Home Page at <http://www.sti.nasa.gov>
- E-mail your question via the Internet to help@sti.nasa.gov
- Fax your question to the NASA STI Help Desk at (301) 621-0134
- Phone the NASA STI Help Desk at (301) 621-0390
- Write to:
NASA STI Help Desk
NASA Center for AeroSpace Information
7115 Standard Drive
Hanover, MD 21076-1320

NASA/TM-2008-215306



Plan for the Characterization of HIRF Effects on a Fault-Tolerant Computer Communication System

*Wilfredo Torres-Pomales, Mahyar R. Malekpour, Paul S. Miner, and Sandra V. Koppen
Langley Research Center, Hampton, Virginia*

National Aeronautics and
Space Administration

Langley Research Center
Hampton, Virginia 23681-2199

May 2008

Acknowledgments

The authors are grateful for the contributions of the following individuals to the definition and implementation of this test: Celeste M. Belcastro, Eric G. Cooper, Jay Ely, Dr. Oscar R. Gonzalez, Dr. W. Steven Gray, John J. Mielnik, Jr., Truong X. Nguyen, Maria Theresa Salud, and Laura J. Smith.

Available from:

NASA Center for AeroSpace Information (CASI)
7115 Standard Drive
Hanover, MD 21076-1320
(301) 621-0390

National Technical Information Service (NTIS)
5285 Port Royal Road
Springfield, VA 22161-2171
(703) 605-6000

Abstract

This report presents the plan for the characterization of the effects of high intensity radiated fields on a prototype implementation of a fault-tolerant computer communication system. Various configurations of the communication system will be tested. The prototype system is implemented using off-the-shelf devices. The system will be tested in a closed-loop configuration with extensive real-time monitoring. This test is intended to generate data suitable for the design of avionics health management systems, as well as redundancy management mechanisms and policies for robust distributed processing architectures.

Table of Contents

1. Overview	1
2. Test Articles	2
2.1. Functional Systems.....	2
2.2. Physical Device	4
3. System Monitoring	4
4. HIRF Environment	7
4.1. Reverberation Chamber Description	7
4.2. Test Facility	7
4.3. Measurement Method	8
5. Test Specification	10
5.1. Hardware Configurations	10
5.2. Device Positions Inside The Test Chamber	11
5.3. Radiation Modulations	11
5.4. HIRF Susceptibility Threshold Characterization.....	12
5.5. Ranking of Nodes and Positions.....	13
5.6. HIRF Effects Characterization	15
6. Test Automation	16
7. Health Checks.....	29
8. Shielding and Grounding.....	29
9. Equipment Layout	30
References	35
Acronyms	36

1. Overview

One of the objectives of the Integrated Vehicle Health Management (IVHM) project of NASA's Aviation Safety Program is to develop failure databases and test capabilities suitable for use in the creation of advanced health-management systems. Safety, cost and performance are addressed as part of this IVHM objective. The IVHM project is also investigating mitigation techniques for failures of avionics systems caused by environmental threats, including electromagnetic interference (EMI) from sources such as lightning and high-intensity radiated electromagnetic fields (HIRF). These environments are of interest because of the potential to cause unexpected and seemingly arbitrary fault manifestations in individual avionics system components, as well as generating simultaneous common-mode faults that can overwhelm current system redundancy management approaches [1, 2]. Among the key challenges of the IVHM project is the development of enabling technologies for the design of large-scale robust and reliable distributed processing architectures for vehicle-wide health assessment and management functions. The work presented here is part of an effort to meet this challenge by focusing on scalable architectural solutions and complementary customizable redundancy management strategies, including fault detection, diagnosis and reconfiguration elements, to meet a wide-range of performance and dependability requirements.

The chosen first step in that direction is to assess the robustness of an existing distributed system by exposing it to severe faults caused by environmental disturbances. This report presents a plan for the generation of data suitable for a first-order characterization of the response of an electronic system experiencing faults. In this fault-injection test, the function of specific targeted devices is disrupted by immersing the devices in a controlled HIRF environment. The tests are performed while the devices operate in a closed-loop configuration and are monitored from a protected location. The system selected for this test is an open-source-based prototype of the communication system of the Scalable Processor-Independent Design for Extended Reliability (SPIDER) architecture concept developed at Langley Research Center (LaRC) under a previous project [3]. This type of platform is essential for this test over proprietary systems because proprietary systems typically provide little or no visibility into their internal operations and tend to be difficult and costly to instrument. Additionally, when proprietary systems are used, the experimental data and analysis results normally cannot be openly shared with the wider research community, thus limiting the potential benefit of the test.

SPIDER is a concept for a family of general-purpose fault-tolerant processing architectures that provides a flexible set of architectural solutions capable of satisfying a wide range of performance and reliability requirements, while preserving a consistent interface to applications. The SPIDER architecture consists of processing elements (PEs) executing the applications and high-level system functions, and the Reliable Optical Bus (ROBUS) data communication system, which provides guaranteed basic services that support PE-level services. The goals of the ROBUS design are to reduce the computational burden on the processing elements, to implement the basic distributed protocols in the way they are most effective (i.e., in hardware), and to provide a simple system abstraction to the PEs for what is an inherently complex distributed processing problem. ROBUS-2, an instance of ROBUS, is a time-division multiple access (TDMA) broadcast data communication system (i.e., a data bus) with medium access control by means of a time-indexed communication schedule. ROBUS-2 provides guaranteed fault-tolerant services to the attached PEs in the presence of a bounded number of internal faults. These services include message broadcast (Byzantine Agreement), dynamic communication schedule update, time reference (clock synchronization), and distributed diagnosis (group membership). ROBUS-2 also features fault-tolerant startup and restart capabilities. ROBUS-2 tolerates internal as well as PE faults, and incorporates a dynamic self-reconfiguration capability driven by the internal diagnostic system. ROBUS-2 consists of custom-designed hardware-based ROBUS Protocol Processors (RPPs)

implementing the ROBUS-2 functionality, and a lower-level physical communication network interconnecting the RPPs. A COTS-based laboratory prototype implementation of ROBUS-2 will be used for this test. Additional information about ROBUS-2 can be found in [4] and [5]. The source code for the ROBUS-2 RPP is publicly available under an open-source license agreement on the Internet at [8].

The objective of the test described here is to characterize the effect of a HIRF environment on the behavior of the ROBUS-2 system and its components. Different system configurations will be tested with variations on the communication data rate, the degree of redundancy, and the number of targeted system components. The characterization will consider the effects at the interfaces to the PEs, at the interfaces of internal system components, and on the state of the communication system. Of special interest is determining the severity of component faults and assessing the robustness of the system to multiple simultaneous faults. We would like to identify weaknesses in the design of ROBUS-2 and desirable features for more robust communication systems. The test results will also contribute to the development of redundancy management mechanisms and policies for robust processing architectures.

2. Test Articles

Figure 1 shows the ROBUS topology. The bus has a redundant active-star architecture with the Bus Interface Units (BIUs) serving as the bus access ports, and the Redundancy Management Units (RMUs) providing connectivity as network hubs. The network between BIUs and RMUs forms a complete bipartite graph in which each node is directly connected to every node of the opposite kind. All the communication links are bidirectional.

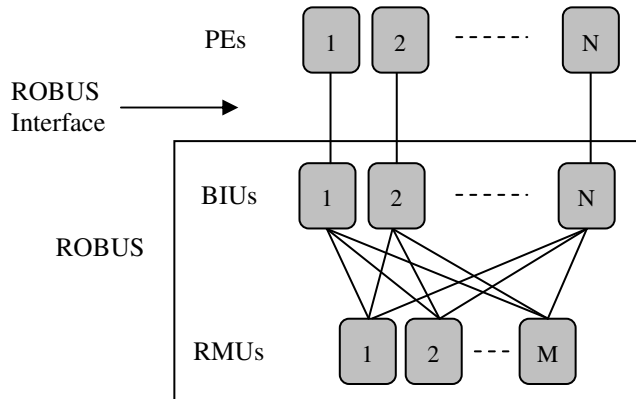


Figure 1: Generic ROBUS Topology

At the interface to the PEs, ROBUS behaves as a shared-medium communication bus with a time-division multiple access (TDMA) channel access pattern. Thus, one way of viewing ROBUS is as a distributed fault-tolerant communication hub.

2.1. Functional Systems

Three different ROBUS configurations will be used in this test: a 4x2 system (i.e., with 4 BIUs and 2 RMUs), a 4x3 system, and a 4x4 system. Figure 2 illustrates these configurations. The **ROBUS 4x2** system has two independent communication paths between every pair of BIUs and can tolerate at most one faulty RMU at any given time. The **ROBUS 4x3** system has three independent paths between every

pair of BIUs and can tolerate one arbitrarily faulty active RMU, and no more than two simultaneously faulty RMUs. The **ROBUS 4x4** system has four independent paths between every pair of BIUs. A 4x4 configuration can tolerate one active arbitrarily faulty RMU, two arbitrarily faulty RMUs if one of them has been diagnosed (and thus isolated from the rest of the system), and no more than three simultaneously faulty RMUs. The ROBUS 4x2, ROBUS 4x3 and ROBUS 4x4 systems can tolerate the same number of faulty BIUs. To enable the performance of some useful work at the PEs, at least two PEs must be able to communicate with each other. A ROBUS system with at least two properly working BIUs can tolerate one active arbitrarily faulty BIU, and no more than two arbitrarily faulty BIUs if one of them has been diagnosed. Each communication system will be tested while interacting with four independent PEs. The three ROBUS configurations are tolerant to faults at the PEs and at the links between the PEs and the communication system.

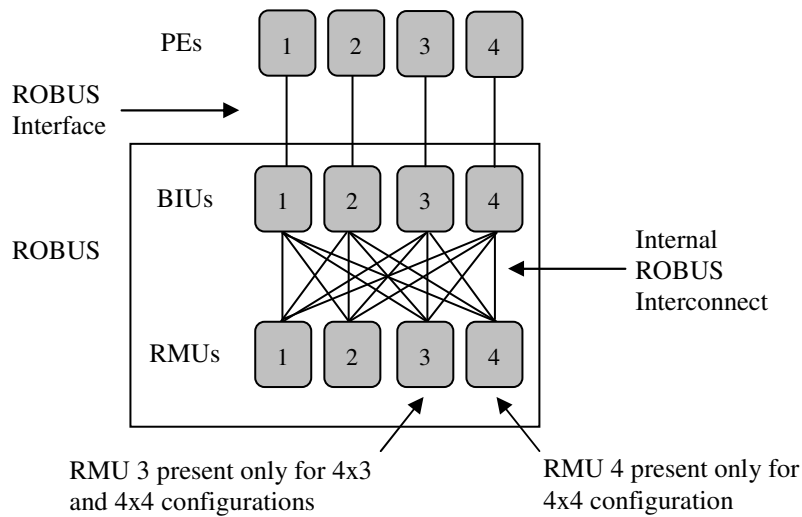


Figure 2: ROBUS Configurations

A **simplex** (i.e., non-redundant) **hub** will also be used in this test. The hub is functionally equivalent to ROBUS at the interface to the PEs. This system will serve as a reference to assess the effectiveness in a HIRF environment of ROBUS with its current redundancy management design. Figure 3 shows the topology of the communication system with the simplex hub.

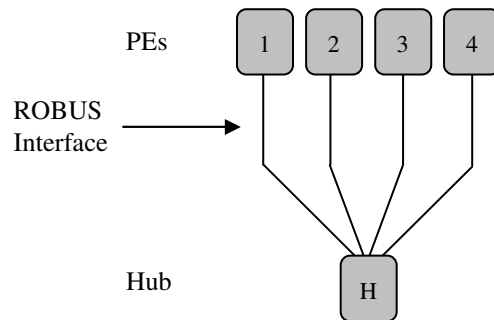


Figure 3: Simple Hub Configuration

2.2. Physical Device

The reconfigurable SPIDER prototyping platform (RSPP) developed for NASA by Derivation Systems, Inc. (DSI) under a phase III SBIR contract will be used to implement the communication systems to be tested. The RSPP is a Field Programmable Gate Array (FPGA) based development system for the design and testing of SPIDER prototypes. The architecture is a scalable modular system composed of individual RSPP nodes interconnected with point-to-point fiber optic links. An RSPP node is a PC/104-plus computer system consisting of the following hardware components.

- **PF3100-2V3000 PC/104+ FPGA Module:** PF3100 with the Xilinx Virtex-II XC2V3000 (3 million gate) FPGA.
- **PFBR104 PC/104 Fiber Optic Transceiver Module:** Interfaces with the PF3100 over the PF3100 IO connector and provides four Agilent HFBR-5905 fiber optic transceivers. Each RSPP node has two PFBR104 modules providing a total of 8 fiber optic IO channels.
- **PC/104+ CPU Module:** The PC/104+ CPU module is a Lippert CRR2 with a 300MHz Pentium class processor, 64MB SDRAM, 256MB Compact Flash, 10/100 Ethernet, VGA, Keyboard, RS232 serial port, parallel port, USB port, and cables. The White Dwarf Linux operating system is installed on the CPU module.
- **PC/104 Power Supply:** A 75 Watt, DC-DC 10A PC/104 power supply is used to provide conditioned power to the internal electrical components of the RSPP node.
- **PC/104 Fan Module:** A fan module provides airflow inside the enclosure to provide cooling of the internal components by providing even heat distribution to avoid hot-spots.
- **PC/104 Enclosure:** A PC/104 enclosure is used to provide packaging as well as EMI shielding for the RSPP node electrical components. The enclosure is made from high-grade extruded aluminum and incorporates a railed card cage subassembly for the electronic components. Endcaps on either end of the enclosure provide access to the internal components, and are machined with cutouts for the various connectors on the RSPP node. Standard PC ports including video, keyboard, mouse, serial, parallel, USB, Ethernet, and power are provided. In addition, eight fiber optic bulkhead adapters are fitted on the endcaps to provide the maximum number of fiber optic channels that can be configured on a single RSPP node.

Figure 4 shows two views of an RSPP node. Each node requires 24 V DC input power and has a 15-ft. power cable with the shield attached to the connectors at both ends. The enclosure is grounded through the power cable shield. The RSPP nodes do not require external cooling. Fiber optic cables of 60 meters (196 feet) in length (to approximate the length of wiring in actual aircraft installations) are used for point-to-point data communication between nodes. For this test, the BIUs, RMUs, and the simplex hub will be implemented on separate RSPP nodes. The four PEs will be implemented on one RSPP node as independent hardware functions.

3. System Monitoring

The communication systems to be tested operate at a 300 Hz cycle rate. In normal operation, with no

faults, each system will process exactly the same data, execute exactly the same operations, and produce exactly the same results in each cycle. This fact will be leveraged in the system monitoring functions. Each system will be monitored in real-time by the PEs and by embedded observers that collect state data from the nodes and relay it to remote monitors. In addition, the messages transmitted by a selected BIU or RMU will be monitored during some of the tests of the ROBUS 4x4 system.

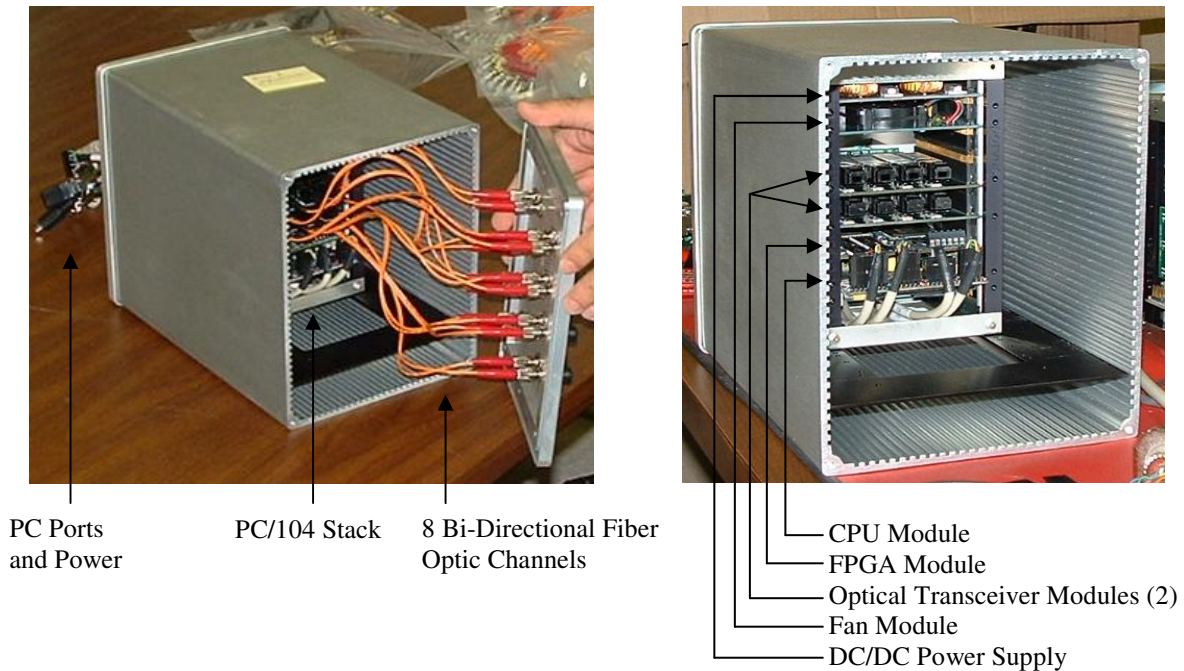


Figure 4: RSPP Node

The **Processing Elements** (PEs) designed for this test serve four functions. First, a PE emulates the behavior of a real processor in its interaction with the communication system. A PE synchronizes and tracks the state of the BIU (or the simplex hub) to ensure proper communication between the two. In normal operation, the communication between the PEs and the bus is time-triggered and highly deterministic. Second, a PE performs error detection on the communication observed at its respective bus interface port. Each PE sends the same messages over the bus during each cycle and checks each received message for timing and content. Third, the PEs forward their observations to a common bus analyzer (see HFA below). Fourth, during each cycle each PE builds a record of its status and observations that is then used for overall system health monitoring (see SHM below) and post-test analysis.

The **Hub Fault Analyzer** (HFA) combines the observations from the four PEs to assess the behavior of the communication system in real-time. The HFA classifies each observation per the categories of a hybrid fault model based on error detection, symmetry, and correctness of received messages. At the end of each communication system cycle, the HFA outputs a record with the results for the cycle. This record is used for overall system health monitoring (see SHM below) and post-test analysis.

The **Node Monitors** record the state of communication system nodes (BIUs, RMUs, or simplex hub). Each time a node makes a Minor Mode transition (see [4]), a record is generated containing the

operational mode, current diagnostic results, and the status of each communication port. This record is used for overall system health monitoring (see SHM below) and post-test analysis.

The **Node Fault Analyzer** (NFA), used in some tests of the ROBUS 4x4 system, combines the observations from four nodes about a particular node of the opposite kind (i.e., four BIUs observing one RMU, or four RMUs observing one BIU) to assess the behavior of the observed node. The NFA uses the same classification functions as the HFA. At the end of each communication system cycle, the NFA outputs a record with the results for the cycle, which is then used for overall system health monitoring (see SHM below) and post-test analysis.

The **System Health Monitor** (SHM) is a generic monitoring function used for real-time assessment of the health of the communication system. Instances of this function are used with each PE, the HFA, each state monitor, and the NFA. Each SHM compares the data records generated by its corresponding function against the records expected during normal system operation and a system health assessment is made based on the timing and content of the records. Figure 5 shows the state transition graph for the SHM. After a reset, a good record (i.e., with expected content) must be received within the Startup Timeout delay, otherwise a system failure will be declared. When the first good record is received, the SHM transitions to the Recovering state, where it will remain until stable good operation is confirmed or a failure to return to normal operation is declared. The SHM will remain in the Trusted state as long as good records are generated by the monitored function.

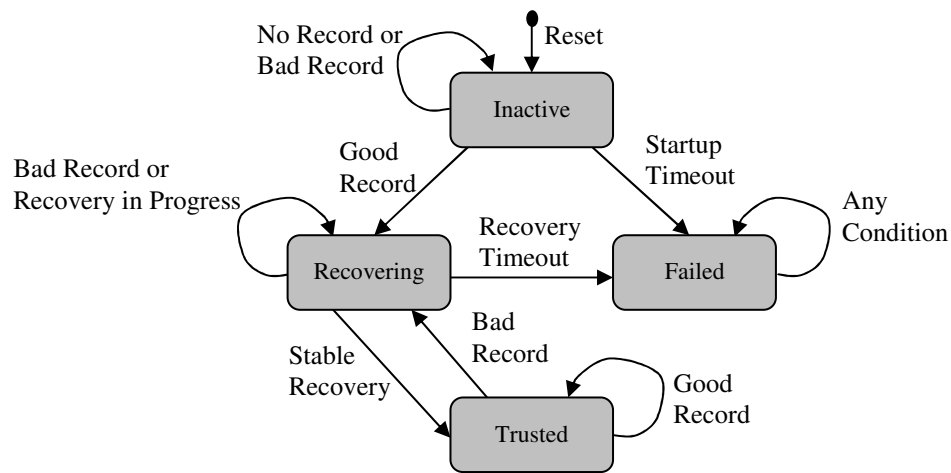


Figure 5: SHM State Transition Graph

For this test, the SHM Startup Timeout is set to 30.0 seconds, the Recovery Timeout is set to 6.0 seconds, and the Stable Recovery timeout is set to 0.5 seconds.

The system monitoring functions will be implemented using two RSPP nodes referred to as the PE Emulator and the Bus Monitor. The **PE Emulator** includes the PEs, HFA, and NFA with their individual SHM modules. The **Bus Monitor** includes a state monitor with an SHM module for each communication system node. The PE Emulator and the Bus Monitor are also used for data collection.

4. HIRF Environment

The test articles will be subjected to a radiated susceptibility testing process. The process, based on RTCA/DO-160D guidelines [6], incorporates the use of a reverberation chamber (RC), RF measurement instrumentation, specialized control and data acquisition software, and the generation and use of calibration data. The test articles will be exposed to radiated electromagnetic (EM) fields from all sides.

4.1. Reverberation Chamber Description

A RC is an electrically conductive shielded enclosure used for generating an electromagnetic (EM) environment for radiated susceptibility and emissions testing. The operational concept is similar to a very large microwave oven. Theoretically, a reverberation chamber is modeled as a large cavity resonator characterized by three-dimensional stationary wave patterns (i.e., resonance modes) at resonant frequencies determined by the dimensions of the chamber. When a radiated field at a resonant frequency enters the cavity, it is reflected back and forth between the walls with low energy loss, and additional energy entering the cavity reinforces the standing wave and increases its intensity. This resonance phenomenon allows the generation of high intensity electromagnetic fields with relatively low input power. However, it has the disadvantage that the spatial distribution of the field is not homogeneous. In practice, a transmit antenna is used to emit RF energy inside the chamber setting up a complex field structure within the chamber. Rotating mechanical stirrers then “mix” the energy, effectively changing the boundary conditions and creating new complex field structures. When sampled over time, this stirring results in a statistically uniform and isotropic test environment.

Reverberation chambers can be operated as either mode-stirred or mode-tuned. During mode-stirring the stirrers continuously rotate at a set rate. Mode-tuning requires the stirrers to be incrementally stepped through a complete rotation with a set dwell time applied at each step. In either case, one complete stirrer rotation will result in environment test samples that are statistically isotropic, uniform, and randomly polarized. Therefore, the test articles are exposed to radiation from all aspect angles and polarizations, thus eliminating the need to move or rotate it. Mode-stirring was chosen for this application because it is easier to implement and significantly reduces test time.

A reverberation chamber is associated with a lowest usable frequency (LUF). The chamber size and geometry contribute to the generation of a sufficient number of modes to ensure adequate field mixing and uniformity. Generally, larger chambers have a lower LUF.

RCs offer several advantages, such as field uniformity and repeatability, the ability to generate high field levels efficiently with less power, reduced test time, and a screened environment with no ambient signals. Disadvantages include loss of polarization and directivity data, and some difficulty correlating time-critical susceptibilities with RF environment.

4.2. Test Facility

Testing will be conducted in the NASA LaRC High Intensity Radiated Fields (HIRF) Laboratory. Figure 6 is a diagram of the layout of the facility which consists of five separate steel chambers. Chambers A, B, and C are reverberation chambers used for radiated emissions and susceptibility testing. Chambers D and E are used as an Amplifier Room and Control Room, respectively. Figure 6 also shows the LUF for each of the chambers. The HIRF Lab chambers were characterized by the National Institute of Standards and Technology (NIST), and demonstrated to have a high level of field uniformity [7]. The facility has the capability to perform distributed testing using two or three of the co-located RCs, which

allows for the simultaneous testing of multiple system components by generating a different radiated environment in each chamber.

Chamber A will be used for this application because the frequency range and power requirements specified in the test plan easily fit within the facility’s capabilities. The HIRF Lab has the resources to operate Chamber A at frequencies up to 18 GHz and at field intensities up to 1500 V/m.

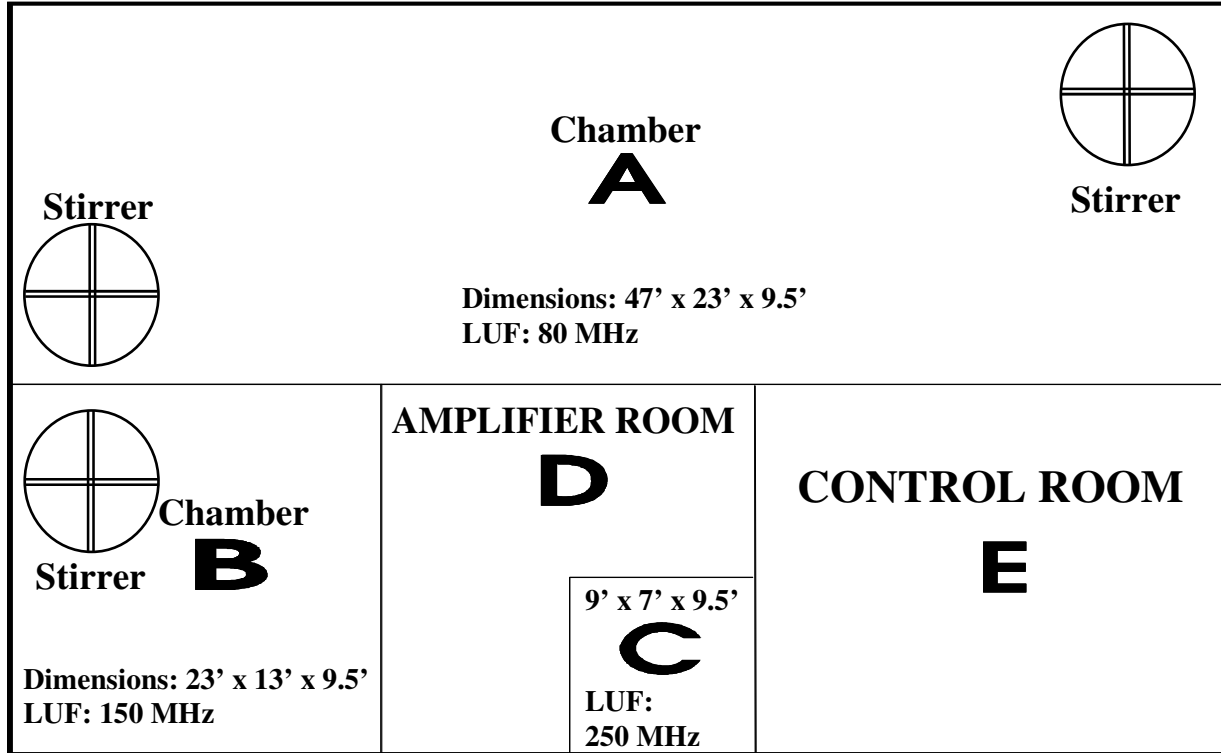


Figure 6: NASA LaRC High Intensity Radiated Fields Laboratory

4.3. Measurement Method

The HIRF Lab reverberation chamber will be operated and calibrated based on RTCA/DO-160D Change 1 guidelines, but with modifications to accommodate mode-stirring. A typical test configuration is illustrated in Figure 7 showing Chamber A, the Amplifier Room (D), the Control Room (E), and test equipment. RC calibration requires transmitting a known input power into the chamber with stirrers rotating. Some of the input power will be lost due to absorption by the chamber, test devices, and antennas. Receive power is measured with a spectrum analyzer in maximum-hold mode. The calibration factor is then determined from the ratio of the known input power to the peak measured receive power. To determine the chamber calibration factor (CF) the following calculation is used [6].

$$CF_{(dB)} = 10 \cdot \log_{10}(8\pi/\lambda^2) + P_{MaxRec(dBm)} - P_{Input(dBm)} \quad (1)$$

where $P_{Input(dBm)}$ denotes the known input power in units of dBm, $P_{MaxRec(dBm)}$ is the measured maximum receive power in units of dBm over a complete stirrer rotation, and λ denotes the frequency wave length. (A dB is a logarithmic measurement unit that expresses the magnitude of a physical quantity relative to a

reference level. The magnitude P of a quantity expressed in dB's relative to magnitude r is defined as $P_{dB} = 10 \bullet \log_{10}(P/r)$, where $\log_{10}()$ is the logarithm with base 10. A dBm is a unit of power in dB relative to 1 mW.)

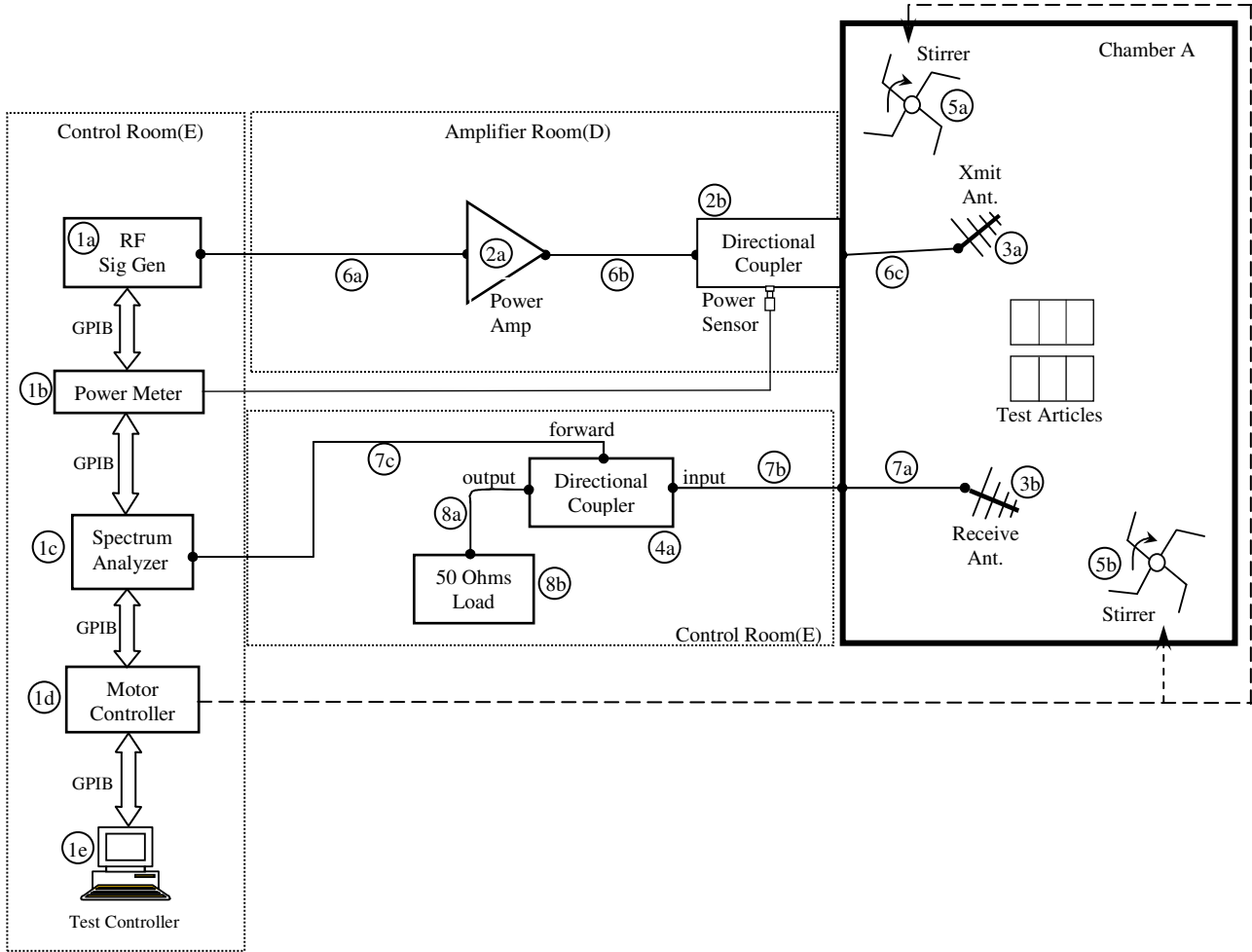


Figure 7: Reverberation Chamber Test Setup illustrating Chamber A, Control Room (E), Amplifier Room (D), and Equipment.

Once the chamber calibration factor is known, a test input power can be calculated that will produce a required electric field level (V/m) inside the chamber using the following.

$$P_{\text{Input(dBm)}} = 10 \bullet \log_{10}(E^2 / 377) + CF_{(dB)} + 30 \text{ dB}, \quad (2)$$

where $P_{\text{Input(dBm)}}$ denotes the input power in dBm at transmit antenna, E is the required electric field in V/m, and $CF_{(dB)}$ is the chamber calibration factor in dB.

As illustrated in Figure 7, forward power from the amplifier is measured using a power meter and peak power RF sensor connected to the forward port of the directional coupler. The input power at the antenna is then related to the measured forward power at the meter when corrected for cable losses (6c) and coupling factor.

The receive path is measured between the receive antenna and the spectrum analyzer and includes cables (7a, 7b & 7c) and a directional coupler (4a). Receive path losses and gains are applied to the maximum power measured at the spectrum analyzer to determine the maximum receive power at the receive antenna.

Measurements can be affected by uncertainties in the RC and the measurement instruments. NIST's characterization of Chamber A [7] indicates uniformity uncertainties of +/- 4 dB at 100 MHz and +/-2 dB at frequencies of 200 MHz and above. Test instrumentation was calibrated to accuracies of +/- 2 dB for the spectrum analyzer, and 0.5 dB or less for the power meter and RF signal generator.

5. Test Specification

The design of ROBUS-2 is supported by formal fault-tolerance theoretical results and design analysis and is based on a set of assumptions about the number, timing and severity of manifestations of active faults [4]. The design of the system re-initialization strategy of ROBUS-2, which is triggered when the system experiences multiple coincident faults beyond the guaranteed-performance capacity of its fault handling mechanisms, is based on the assumption that such events can only be caused by rare external disturbances of known bounded duration. As the purpose of this test is to assess the robustness of the ROBUS-2 system, and given the highly deterministic (and thus uninteresting) behavior of ROBUS-2 when its timing design assumptions are satisfied, this test is deliberately specified such that the duration of the HIRF exposures are longer than assumed in the design of the system. Furthermore, the test specification takes advantage of the known fault-tolerance degree of ROBUS-2 to characterize the behavior of individual ROBUS nodes while operating in their normal system configuration with absolute certainty that the tested node will have no significant impact on the behavior of the rest of the system.

The test consists of two parts. The purpose of the first part, called the **HIRF Susceptibility Threshold Characterization (HSTC)**, is to determine the change in the susceptibility threshold (i.e., the minimum field strength to cause an upset) of the RSPP nodes as a function of test frequency, the actual radiated physical node, the location of a node inside the test chamber, and the radiation pattern that a node is exposed to. The data from the HSTC will be used in the second part, called the **HIRF Effects Characterization (HEC)**, to determine the range of field strengths and the set of frequencies for testing various hardware configurations to characterize the effects of the radiation on the targeted devices.

5.1. Hardware Configurations

Table 1 lists the hardware configurations available for this test. There will be two versions of each communication system: a low-speed version with a 3.2 Mbps (mega-bits per second) data rate, and a high-speed version at 12.8 Mbps. Testing versions with different data rates will serve to examine the dependence between the data rate and the response of the system to radiated fields. The ROBUS 4x2 and 4x3 systems use the same BIU and RMU implementations as the ROBUS 4x4 system. The only physical difference between these systems is the actual number of RMUs used. ROBUS-2 has the capability to automatically detect missing nodes and reconfigure its state accordingly.

Four ROBUS 4x4 system configurations will be available in which only one node is targeted. The purpose of these configurations is to characterize the node fault manifestations within ROBUS. Such data is important for the design of effective redundancy management strategies. These configurations will be the only ones using the NFA monitoring function.

Table 1: Available Hardware Configurations

Hardware Configuration	Communication System	Data Transfer Rate	Radiated Components (Targets)
HC1	Simplex Hub	Low	Hub
HC2	Simplex Hub	High	Hub
HC3	ROBUS 4x4	Low	RMU 1
HC4	ROBUS 4x4	Low	BIU 1
HC5	ROBUS 4x2	Low	RMU 1
HC6	ROBUS 4x4	High	RMU 1
HC7	ROBUS 4x4	High	BIU 1
HC8	ROBUS 4x2	High	RMU 1
HC9	ROBUS 4x2	Low	ROBUS 4x2
HC10	ROBUS 4x3	Low	ROBUS 4x3
HC11	ROBUS 4x4	Low	ROBUS 4x4
HC12	ROBUS 4x2	High	ROBUS 4x2
HC13	ROBUS 4x3	High	ROBUS 4x3
HC14	ROBUS 4x4	High	ROBUS 4x4

The ROBUS 4x2 configurations with one targeted RMU are intended to characterize the response of the system when the number of non-faulty redundant components of a particular kind is reduced to the minimum.

The remaining configurations targeting the whole communication system in each case are meant to assess the relative effectiveness of the communication systems in handling HIRF-induced faults. For these configurations, their fault handling effectiveness will be assessed at the PE interfaces. Configurations of ROBUS 4x2, 4x3 and 4x4 systems can also be analyzed from the perspective of their internal state transitions in response to HIRF-induced faults.

5.2. Device Positions Inside The Test Chamber

Figure 8 shows the options for positioning devices inside the test chamber. The locations are identified by the numbers 1 through 8 as indicated. At each location there is a non-conductive foam block or table intended to support at most one RSPP node elevated above the chamber floor. The devices can be placed at these locations such that the distance between any two devices and between the devices and the stirrers, chamber walls, and antennas is at least one-half wavelength at the lowest test frequency (i.e., 1.5 meters at 100 MHz). This separation is intended to reduce the disturbance to the local radiation characteristics caused by other items inside the chamber.

5.3. Radiation Modulations

Various modulations to the chamber RF (radio frequency) input signal will be used in this test. The basic waveform is a continuous (i.e., unmodulated) wave (CW). Pulse modulation will consist of 20 μ s pulses of the test frequency at a 1 kHz pulse rate. A square wave modulated input signal will have a modulation frequency of 1 kHz and a 50% duty cycle. The pulse and square modulations are defined taking into consideration the reverberation chamber time constant and wave modulation recommendations in [6].



Figure 8: Device Positions inside the Test Chamber

Additionally, it is known that due to the reverberation and stirring of the field inside the test chamber, the targeted devices will experience position and time-dependent field amplitude modulations superimposed on the input RF signal modulation. For completeness, we intend to measure at one or more locations the magnitude of the peak field as a function of stirrer rotation angle.

5.4. HIRF Susceptibility Threshold Characterization

The HSTC is intended to characterize the dependence of the HIRF susceptibility threshold to variations in frequency, physical device, radiation modulation, and position within the test chamber. The HSTC consists of a series of tests as described in Table 2. Hardware configurations HC3 and HC4 will be used for these tests. For HC3 configuration tests, physical RSPP nodes 5 through 8 alternate to perform the targeted RMU1 function as indicated in Table 2. Likewise, for HC4 configuration tests, physical RSPP nodes 1 through 4 will be reprogrammed to perform the BIU 1 function as indicated.

For each test, the desired output is a graph indicating the minimum field strength to cause an upset for each test frequency. The 2-out-of-3 rule described in Section 5 will be used to identify the susceptibility threshold of the targeted device at a particular frequency. The test frequency range is 100 MHz to 1000 MHz with specific frequency values determined by the formula $f_{n+1} = (10^{1/24})f_n$ [6] for a total of 25 frequencies. At each HSTC test frequency, the calibrated peak electric field strength is swept starting at the lowest test field strength and increasing in steps of 20 V/m until the susceptibility threshold or the maximum field strength is reached. For tests with unspecified lowest test field strength in Table 2, the results from preceding tests will be used to determine an appropriate lowest level. Document [6] and recommendations from HIRF Lab personnel were considered in the specification of the field strength ranges. The stirrers will be set to rotate at 10 seconds per revolution. The dwell time at each tested frequency-and-field-strength point will be 30 seconds (i.e., 3 stirrer rotations). Each individual radiation exposure at a particular frequency and field strength is called a **round**.

Table 2: Tests for HIRF Susceptibility Threshold Characterization

HSTC Test Id	Hardware Configuration	Variable of Interest	ROBUS Node	Physical RSPP node	Position	Modulation	Field Range (V/m)
1	HC3	Physical Node	RMU 1	5	5	CW	20 – 300
2	HC4	Physical Node	BIU 1	1	5	CW	Up to 300
3	HC4	Physical Node	BIU 1	2	5	CW	Up to 300
4	HC4	Physical Node	BIU 1	3	5	CW	Up to 300
5	HC4	Physical Node	BIU 1	4	5	CW	Up to 300
6	HC3	Physical Node	RMU 1	6	5	CW	Up to 300
7	HC3	Physical Node	RMU 1	7	5	CW	Up to 300
8	HC3	Physical Node	RMU 1	8	5	CW	Up to 300
9	HC3	Modulation	RMU 1	5	5	Pulse	Up to 500
10	HC4	Position	BIU 1	1	1	CW	Up to 300
11	HC4	Position	BIU 1	2	2	CW	Up to 300
12	HC4	Position	BIU 1	3	3	CW	Up to 300
13	HC4	Position	BIU 1	4	4	CW	Up to 300
14	HC3	Position	RMU 1	6	6	CW	Up to 300
15	HC3	Position	RMU 1	7	7	CW	Up to 300
16	HC3	Position	RMU 1	8	8	CW	Up to 300
17	HC3	Modulation	RMU 1	5	5	Square wave	Up to 400

5.5. Ranking of Nodes and Positions

The results of the HSTC will include the ranking of the physical nodes based on their average field strength susceptibility across the tested frequency range, and also the ranking of the chamber positions based on the average magnitude of the local field strength across the tested frequency range. Both of these ranking will only consider CW modulation tests. Since it is expected that the measured susceptibility threshold of multi-node ROBUS configurations will be dependent on the position assignment of the constituent nodes, the rankings of the physical nodes and positions will be used to try to predetermine the relative susceptibility threshold of the tested communication systems and thus make the comparison of relative fault handling effectiveness as fair as possible. It is known that the peak field intensity at a particular position inside the chamber is highly dependent on the relative alignment of the field stirrers, and that because of this the rankings of the tested nodes and positions based on observed susceptibility thresholds are not reliable. Nevertheless, this approach will be used as it provides a simple, methodical way of deciding how to position multiple nodes inside the chamber.

To enable the ranking of the positions by the local field strength and of the nodes by their

susceptibility to the field, a model has been developed that relates the nominal field strength in the chamber to the magnitude of the disturbance experienced by the internal electronic components of a node. The nominal field strength will be measured by a receive antenna at a fixed position separate from where the nodes will be placed. Although mode stirring will be used in this test, which provides a certain degree of spatial field uniformity, it is expected that the local peak field strength will be different for each of the identified test node positions. It is also expected that each node will have a slightly different susceptibility threshold with respect to the local peak field strength. Equation (3) incorporates these two factors determining the observed susceptibility threshold with respect to the nominal field strength.

$$V^I = W^P \cdot W^S \cdot E \quad (3)$$

Here, V^I is the disturbance voltage experienced by the internal electronic components of a node, W^P is a scaling factor that maps the nominal field strength to the local field strength at a given position, W^S is a scaling factor mapping the local field strength to the magnitude of the disturbance experienced internally by the electronic components of the node, and E is the nominal field strength. Factor W^S is inversely proportional to the shielding effectiveness of a node, such that a lower value of W^S corresponds to a more effective shielding of the node's internal electronic components.

In using equation (3) to rank the nodes and positions, it is assumed that the internal electronic components of all the nodes have the same susceptibility threshold, such that all the nodes experience an upset at the same value of V^I . Differences among the nodes in the value of factor W^S is assumed to be caused by slight variations in manufacturing and layout of the nodes, including wiring. Differences in the value of factor W^P are assumed to be due to limitations of the field stirring mechanism and positioning of the node.

Tests 1 through 8 in Table 2 will measure the nominal susceptibility threshold of the nodes at position 5. W^P is assumed constant for all those tests, and therefore, the differences in the measured susceptibility thresholds of the nodes are due to differences in the value of the W^S factor. Thus, ranking the nodes by their susceptibility threshold consists of sorting the values of their W^S factors. Equation (4), derived using equation (3) for two nodes, x and 5, will be used for this purpose.

$$W_x^S / W_5^S = E_5^S / E_x^S \quad (4)$$

Here, W_x^S is W^S for node x and W_5^S is W^S for reference node 5. E_b^a is the nominal susceptibility threshold of node b at position a . Using equation (4) we can rank the nodes by their susceptibility relative to the susceptibility of node 5 using the measured nominal field strength susceptibility thresholds.

The results of tests 1 through 8 and 10 through 16 in Table 2, where each node is tested at reference position 5 and at one other position, will be used to rank the positions by the local field strength. Specifically, the positions will be ranked by the value of their W^P factors using the susceptibility thresholds measured at each position and at reference position 5 for a particular node. In this case, W^S is held constant and W^P varies. Applying equation (3) for position 5 and for some position y with the same node x , we can derive equation (5).

$$W_y^P / W_5^P = E_x^5 / E_x^y \quad (5)$$

Here, W_y^P is W^P for position y and W_5^P is W^P for reference position 5. From equation (5), a higher susceptibility threshold at position y corresponds to a lower value of scaling factor W_y^P , which indicates

that the local field strength there is lower, as expected. Thus, with this expression we can sort the positions by their local field strength relative to the field strength at position 5 using the measured susceptibility thresholds.

To account for the various test frequencies in the HSTC, the final ranking of nodes and positions will be based on the average ranking for the set of tested frequencies.

5.6. HIRF Effects Characterization

Table 3 lists the tests for the HEC. As shown, low and high susceptibility threshold position assignments will be tested for each hardware configuration. For HC1 and HC2 configurations involving the simplex hub, a physical node and position assignment with average susceptibility threshold (i.e., approximately at the midpoint between the extremes) will also be tested.

For each of these tests and at each tested frequency, the field strength will be incremented first in steps of 20 V/m until the susceptibility threshold level is reached, and then a finer resolution of 10 V/m will be used to more accurately determine the susceptibility threshold. CW will be used for these phases. Once the threshold is determined for a particular test frequency, the HEC part of the test begins.

An HEC round consists of a series of discrete radiation exposures separated by intervals with no radiation. Each radiation exposure is called a **strike**, and each quiet interval after a strike is called a **lull**. Each strike will consist of 5 seconds of continuous unmodulated (CW) radiation. Each lull will also last for 5 seconds. The purpose for the lulls is to allow the targeted system to recover before the arrival of the next disturbance. Each HEC round will last for 200 seconds (i.e., 20 radiation strikes), and the field strength will increment in steps of 10 V/m between rounds. The stirrers will move at 5 seconds per revolution.

The actual test frequencies, field strength ranges, and the position assignments for targeted physical RSPP nodes will be selected based on the results of the HSTC tests. Due to time constraints, it is likely that not all the tests in Table 3 can be carried out. In that case, a subset will be selected taking into consideration time availability and the results of the HSTC tests.

Table 3: Tests for HIRF Effects Characterization

Hardware Configuration	Number of Hardware Position Assignments (Expected relative susceptibility thresholds)
HC1	3 (Low, Average, High)
HC2	3 (Low, Average, High)
HC3	2 (Low, High)
HC4	2 (Low, High)
HC5	2 (Low, High)
HC6	2 (Low, High)
HC7	2 (Low, High)
HC8	2 (Low, High)
HC9	2 (Low, High)
HC10	2 (Low, High)
HC11	2 (Low, High)
HC12	2 (Low, High)
HC13	2 (Low, High)
HC14	2 (Low, High)

6. Test Automation

The Test Control System (TCS) consists of three interconnected computers. The **Test Controller** controls the RF environment inside the test chamber and the power supply for the targeted components. The **PE Emulator** implements the PE, Hub Fault Analyzer, and Node Fault Analyzer functions, and monitors the operation of the communication system under test (SUT) at its interface. The **Bus Monitor** implements the SUT state monitoring function. Figure 9 shows the interconnection topology of the TCS. The Test Controller is the central element of this system, with the PE Emulator and Bus Monitor working as SUT monitoring controllers. The computers communicate via RS-232 serial links. Communication with the tested communication system (i.e., ROBUS or the simplex hub) is via fiber-optic links. A separate computer serves as a data repository and is connected to the PE Emulator and the Bus Monitor via a dedicated Ethernet network.

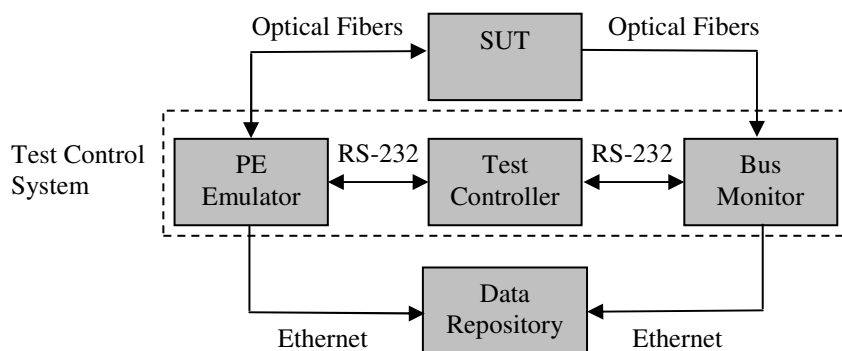


Figure 9: Test Control System Topology

The PE Emulator and Bus Monitor computers are programmed with information about the hardware configuration being tested and the duration of a round, but they do not have information about the test sequences.

The TCS operates in rounds, with the field settings for each execution round corresponding to a point in a field-strength-by-frequency matrix. The execution of a round is enabled by the TCS operators, who are also responsible for monitoring the operation of the system during the round. Each computer is enabled independently. Once enabled, the computers automatically coordinate their actions during a round using the Controller Coordination Protocol (CCP). The CCP is a handshake protocol that enables the test control computers to execute a test round and provides exception-handling capability to ensure that the computers gracefully finish the execution of each round. The TCS operators serve as backup to deal with unexpected situations (e.g., a TCS computer crash).

A TCS execution round consists of two phases: SUT Check and SUT Test. In the SUT Check phase, the TCS powers up the SUT target components and confirms normal operation. The SUT Test phase is where the SUT target components are exposed to the test radiation environment. After the SUT Test phase is complete, the TCS saves the collected data and waits for operator authorization to begin the next round. The TCS execution ends after the last round of a HIRF test is complete.

Figure 10 shows an example of the flow of events for a normal execution of the CCP protocol. A

basic assumption of the protocol is that for each round all the TCS computers are enabled within a time interval of known bounded duration. This is illustrated by the TCS Enable interval in Figure 10.

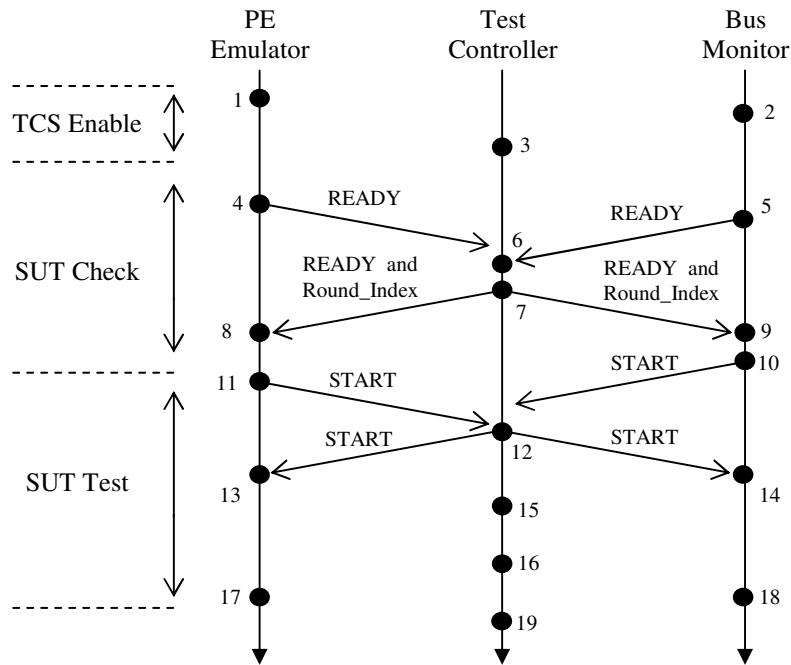


Figure 10: Typical event sequence for the CCP protocol

Description of events in Figure 10:

1. The PE Emulator is enabled by the operator and transitions from state WAIT_CONTINUE to state DELAY_READY.
2. The Bus Monitor is enabled by the operator and transitions from state WAIT_CONTINUE to state DELAY_READY.
3. The Test Controller is enabled by the operator and transitions from state WAIT_CONTINUE to state WAIT_READY.
4. The PE Emulator sends READY and transitions to state WAIT_READY_ECHO.
5. The Bus Monitor sends READY and transitions to state WAIT_READY_ECHO.
6. The Test Controller receives two READY messages.
7. After powering up the SUT target components, the Test Controller broadcasts READY and the Round Index, and then transitions to state WAIT_START.
8. When the PE Emulator receives READY and the Round Index, it enables the local SUT monitoring functions and transitions to state WAIT_SUT_STATUS.

9. When the Bus Monitor receives READY and the Round Index, it enables the local SUT monitoring functions and transitions to state WAIT_SUT_STATUS.
10. When the Bus Monitor confirms that the SUT is operating normally, it sends START and transitions to state WAIT_START_ECHO.
11. When the PE Emulator confirms that the SUT is operating normally, it sends START and transitions to state WAIT_START_ECHO.
12. When the Test Controller receives both START messages, it broadcasts START, starts a delay timer to begin the HIRF radiation, and transitions to state WAIT_HIRF_BEGIN.
13. When the PE Emulator receives START, it starts a round duration timer and begins collecting SUT execution data in state WAIT_ROUND_COMPLETION.
14. When the Bus Monitor receives START, it starts a round duration timer and begins collecting SUT execution data in state WAIT_ROUND_COMPLETION.
15. When the Test Controller's HIRF delay timer expires, the radiation begins and the Test Controller transitions to state WAIT_HIRF_END.
16. The Test Controller ends the radiation and transitions to state WAIT_ROUND_CONTINUE.
17. When the PE Emulator's round duration timer expires, it saves the collected data to the repository and transitions to state SAVE_DATA_RECORDS.
18. When the Bus Monitor's round duration timer expires, it saves the collected data to the repository and transitions to state SAVE_DATA_RECORDS.
19. Round ends for the Test Controller, and it transitions to state ROUND_DECISION.

The READY, START, and STOP messages used in the CCP are mapped to RS-232 messages as indicated on Table 4.

Table 4: CPP message encoding for RS-232 communication

CCP Message	RS-232 Message		
	Decimal	Binary	ASCII
READY	70	0100_0110	F
START	85	0101_0101	U
STOP	90	0101_1010	Z

The RS-232 links are configured as follows.

- Baud Rate 19200
- Message Format 8N1 (8-bit character, no parity, 1 stop bit)
- Flow Control Hardware

The transmission of the Round_Index variable by the Test Controller is implemented as three separate RS-232 messages, each carrying the ASCII code representation of a digit of the value of Round_Index (i.e., each digit is transmitted as a character). The most significant digit is transmitted first.

Table 5 lists execution variables used in the CCP process executed by the Test Controller. There are three test phases defined. During the HSTC test phase, the field strength will be incremented until the susceptibility threshold is reached. The FHSTC (Fine HSTC) test phase determines the susceptibility threshold with the finer field strength resolution. The HEC test phase executes the HEC long duration rounds at or above the susceptibility threshold. The following parameters are used in the definition of the CCP.

- HSTC_Max_Field_Strength = Maximum field strength for HSTC and FHSTC test phases
- HEC_Num_Field_Levels = Number of test field levels for HEC mode
- $N = \max(3, \text{HEC_Num_Field_Levels})$

As the central element of the TCS, the Test Controller is responsible for automatically creating a test log file. A test log entry is made after each round.

Table 5: Execution variables for the Test Controller CCP process

Variable	Data Type	Data Range	Comments
Test_Phase	Enumerated	{HSTC, FHSTC, HEC}	For HSTC tests, HSTC is the only phase. For HEC tests, all the phases apply.
HSTC_Done	Boolean	{FALSE, TRUE}	Flag asserted if no susceptibility is found up to HSTC_Max_Field_Strength
HEC_Done	Boolean	{FALSE, TRUE}	Flag asserted when HEC test phase is complete
Round_Index	Integer	000 - 999	Unique round identifier
Frequency	Real	100.0 - 1000.0 MHz	--
Field_Strength	Real	0.0 – 1000.0 V/m	--
HSTC_Fail_Field_Strength	Real	0.0 - 1000.0 V/m	--
Trial	Integer	1 - N	For 2-out-of-3 rule, and HEC test phase
Round_Result	Enumerated	{Abort, Pass, Fail}	Result of round
Test_Point_Decision	Enumerated	{None, Retry, Pass, Fail}	Decision for the test point.

Table 6 lists the timeout delays used in the Test Controller CCP process. Specific values for the CCP timeout delays will be empirically determined during the integration of the TCS computers.

Table 6: Timeout delays for the Test Controller CCP process

Timeout	Comments
READY_Receive_Delay_Max	Maximum allowed delay for receiving the READY messages from the monitors after the Test Controller is enabled to execute a round.
START_Receive_Delay_Max	Maximum allowed delay to receive the START messages from the monitors after the READY echo is sent by the Test Controller
HIRF_Begin_Delay	Delay by the Test Controller to start the radiation after sending the START echo message
HSTC_Round_End_Delay	Time delay from the beginning of the radiation until the round is complete for the HSTC and FHSTC test phases
HEC_Round_End_Delay	Time delay from the beginning of the radiation until the round is complete for the HEC test phase

Figure 11 shows the rule for deciding what to do after the radiated target components experience errors at a given field strength and frequency test point. This is a 2-out-of-3 rule for confirming susceptibility at a given frequency and field strength. This rule applies to the HSTC and FHSTC test phases.

1. If a target-originated error is not detected during the first round, the target shall be tested at the next field strength level. If a target-originated error is detected during the first round, the round shall be repeated.
2. If a target-originated error is detected during the second round, susceptibility is confirmed. If a target-originated error is not detected during the second round, the round shall be repeated once more.
3. If a target-originated error is detected during the third round, susceptibility is confirmed. If a target-originated error is not detected during the third round, the target shall be tested at the next field strength level.

Figure 11: Rule for determining susceptibility at a given frequency and field strength

Figure 12 lists the CCP process for the Test Controller using pseudo-code and finite state machine (FSM) notation. This process is designed to always return the Test Controller, the RF equipment and the targeted devices inside the chamber to a safe state after every round. The test log files and the field measurements collected by the Test Controller are stored locally during testing and transferred to the repository afterward.

Figure 13 lists the CCP process for the PE Emulator and the Bus Monitor. After every round, the PE Emulator and the Bus Monitor automatically transfer their data files to the test data repository. This process is designed with an auto-continue feature by which the PE Emulator and the Bus Monitor automatically begin the next round if no abnormal conditions are detected by the end of a round. The Test Controller process does not have this feature and requires the operator to manually begin the next round. This combination simplifies and expedites the execution of the test, while allowing the operator to always maintain control and safety during the test.

Table 7 lists the timeout delays in the CCP process of the PE Emulator and the Bus Monitor. The

operator can select one of two available round duration delays, one for the HSTC and FHSTC test rounds and another for the HEC rounds.

Table 7: Timeout delays in the CCP process for the PE Emulator and the Bus Monitor

Timeout	Comments
READY_Send_Delay	Delay to send the READY message after the round execution is enabled
READY_Echo_Delay_Max	Maximum allowed delay to received the READY message echo from the Test Controller after sending the READY message
START_Echo_Delay_Max	Maximum allowed delay to received the START message echo from the Test Controller after sending the START message
Round_Completion_Delay_1	Option 1 for the duration of the round
Round_Completion_Delay_2	Option 2 for the duration of the round

Figure 12: CCP Process for the Test Controller

```

Initialize: Round_Index, Frequency, Field_Strength, Trial, Max_HSTC_Field_Strength
Open log file
Test_Phase = HSTC
HSTC_Done = FALSE
HEC_Done = FALSE
Previous_Round_Stopped = TRUE
Current_State = WAIT_CONTINUE
Power down SUT target components
FSM(Current_State)
  WAIT_CONTINUE:
    if (Operator_Input = DONE) or (HSTC_Done = TRUE) or (HEC_Done = TRUE),
      Close log file
      Exit
    elsif (Operator_Input = CONTINUE),
      Set up test equipment for round: Frequency, Field_Strength, Strike Pattern
      if (Previous_Round_Stopped = TRUE)
        Clear PE_Emulator_Message and Bus_Monitor_Message buffers
      end if
      Previous_Round_Stopped = TRUE
      Start Timeout1(READY_Receive_Delay_Max)
      Current_State = WAIT_READY
    else
      Current_State = WAIT_CONTINUE
    end if

  WAIT_READY:
    if (Operator_Input = STOP) or (Timeout1) or
      ((PE_Emulator_Message != no_message) and
      (PE_Emulator_Message != READY)) or
      ((Bus_Monitor_Message != no_message) and
      (Bus_Monitor_Message != READY)),
      Broadcast STOP message
      Round_Result = Abort
      Current_State = ROUND_DECISION
    elsif (PE_Emulator_Message = READY) and
      (Bus_Monitor_Message = READY),
      Power up SUT target components
      Broadcast READY message
      Broadcast Round_Index
      Start Timeout2(START_Receive_Delay_Max)
      Current_State = WAIT_START
    else
      Current_State = WAIT_READY
    end if

  WAIT_START:
    if (Operator_Input = STOP) or (Timeout2) or
      ((PE_Emulator_Message != no_message) and
      (PE_Emulator_Message != START)) or
      ((Bus_Monitor_Message != no_message) and
      (Bus_Monitor_Message != START)),
      Broadcast STOP message
      Round_Result = Abort

```

Figure 12: CCP Process for the Test Controller (continued)

```

    Current_State = ROUND_DECISION
elseif (PE_Emulator_Message = START) and (Bus_Monitor_Message = START),
    Broadcast START message
    Start Timeout3(HIRF_Begin_Delay)
    Current_State = WAIT_HIRF_BEGIN
else
    Current_State = WAIT_START
end if

```

WAIT_HIRF_BEGIN:

```

if (Operator_Input = STOP) or
    (PE_Emulator_Message != no_message) or
    (Bus_Monitor_Message != no_message),
    Broadcast STOP message
    Round_Result = Abort
    Current_State = ROUND_DECISION
elseif (Timeout3),
    Begin HIRF Radiation
    If (Test_Phase = HEC)
        Start Timeout4(HEC_Round_End_Delay)
    else
        Start Timeout4(HSTC_Round_End_Delay)
    end if
    Current_State = WAIT_HIRF_END
else
    Current_State = WAIT_HIRF_BEGIN
end if

```

WAIT_HIRF_END:

```

if (Operator_Input = STOP),
    End HIRF radiation
    Broadcast STOP message
    Round_Result = Abort
    Current_State = ROUND_DECISION
elseif (PE_Emulator_Message != no_message) or
    (Bus_Monitor_Message != no_message),
    End HIRF radiation
    Broadcast STOP message
    Round_Result = Fail
    Current_State = ROUND_DECISION
elseif ((Test_Phase = HEC) and (HEC HIRF Round Finished)) or
    ((Test_Phase != HEC) and (HSTC HIRF Round Finished))
    End HIRF radiation
    Current_State = WAIT_ROUND_END
else
    Current_State = WAIT_HIRF_END
end if

```

WAIT_ROUND_END:

```

if (Operator_Input = STOP),
    Broadcast STOP message
    Round_Result = Abort
    Current_State = ROUND_DECISION

```

Figure 12: CCP Process for the Test Controller (continued)

```

elseif (PE_Emulator_Message != no_message) or
  (Bus_Monitor_Message != no_message),
  Broadcast STOP message
  Round_Result = Fail
  Current_State = ROUND_DECISION
elseif (Timeout4),
  Previous_Round_Stopped = FALSE
  Round_Result = Pass
  Current_State = ROUND_DECISION
else
  Current_State = WAIT_ROUND_END
end if

ROUND_DECISION:
if (Round_Result != Pass),
  Power down SUT target components
end if

// Test Point, Field Strength, and Test Phase Decision
if (Test_Phase = HSTC) or (Test_Phase = FHSTC),
  // Test Point Decision for HSTC and FHSTC (2-out-of-3 rule)
  if (Round_Result = Abort),
    Test_Point_Decision = None
  else
    if (Trial = 1),
      if (Round_Result = Pass),
        Test_Point_Decision = Pass
      else
        Test_Point_Decision = Retry
      end if
    elseif (Trial = 2),
      if (Round_Result = Pass),
        Test_Point_Decision = Retry
      else
        Test_Point_Decision = Fail
      end if
    else
      if (Round_Result = Pass),
        Test_Point_Decision = Pass
      else
        Test_Point_Decision = Fail
      end if
    end if
  end if

  // Make log file entry
  Log file entry: Round_Index, Frequency, Field_Strength, Trial,
                 Round_Result, Test_Point_Decision, Test_Phase

  // Set Trial number and Round Index
  if (Test_Point_Decision = Pass) or (Test_Point_Decision = Fail),
    Trial = 1
  end if
end if

```

Figure 12: CCP Process for the Test Controller (continued)

```

    Round_Index ++
elseif (Test_Point_Decision = Retry)
    Trial ++
    Round_Index ++
end if

// Decide next Test_Phase and Field_Strength
if (Test_Phase = HSTC) and (Test_Point_Decision = Pass),
    if (Field_Strength = HSTC_Max_Field_Strength),
        HSTC_Done = TRUE
    else
        Field_Strength = HSTC_Next_Field_Strength(Field_Strength)
    end if

elseif (Test_Phase = HSTC) and (Test_Point_Decision = Fail),
    // Save current HSTC field strength
    HSTC_Fail_Field_Strength=Field_Strength

    // Get first FHSTC field strength
    Field_Strength = FHSTC_First_Field_Strength(Field_Strength)

    // Go to FHSTC Phase
    Test_Phase = FHSTC

elseif (Test_Phase = FHSTC) and (Test_Point_Decision = Pass),
    // Get next FHSTC field strength
    Field_Strength = FHSTC_Next_Field_Strength(Field_Strength)

    // If next FHSTC field strength is equal to the latest one of HSTC
    // (with test point decision of Fail), do not retest there and go directly to HEC
    If (Field_Strength = HSTC_Fail_Field_Strength),
        Field_Strength = HEC_First_Field_Strength(
            HSTC_Fail_Field_Strength)

        Test_Phase = HEC
    end if

elseif (Test_Phase = FHSTC) and (Test_Point_Decision = Fail),
    // Get first HEC test point and go to HEC phase
    Field_Strength = HEC_First_Field_Strength(Field_Strength)
    Test_Phase = HEC
end if

else
    // For HEC
    // Test Point Decision
    if (Round_Result = Abort),
        Test_Point_Decision = None
    elseif (Round_Result = Pass),
        Test_Point_Decision = Pass
    else
        Test_Point_Decision = Fail
    end if
end if

```

Figure 12: CCP Process for the Test Controller (continued)

```
// Make log file entry
Log file entry: Round_Index, Frequency, Field_Strength, Trial,
                Round_Result, Test_Point_Decision, Test_Phase

// Decide next Test_Phase and Field Strength
if (Test_Point_Decision != None)
  if (Trial = HEC_Num_Field_Levels),
    // Done with HEC.
    HEC_Done = TRUE
    Trial = 1
    Round_Index ++
  else
    // Continue with HEC
    Trial ++
    Round_Index ++
    Field_Strength = HEC_Next_Field_Strength(Field_Strength)
  end if
end if

Current_State = WAIT_CONTINUE
```

Figure 13: CCP Process for the PE Emulator and the Bus Monitor

```

Load local SUT-interface functions
Auto_Continue = FALSE
Current_State = WAIT_CONTINUE
FSM(Current_State)
  WAIT_CONTINUE:
    if (Auto_Continue = FALSE) and
      if (Operator_Input = DONE),
        Exit
      elsif (Operator_Input = CONTINUE_1) or (Operator_Input = CONTINUE_2),
        Disable and reset local SUT-interface functions
        Clear Test_Controller_Message buffer
        Auto_Continue = FALSE
        if (Operator_Input = CONTINUE_1)
          Round_Completion_Delay = Round_Completion_Delay_1
        else
          Round_Completion_Delay = Round_Completion_Delay_2
        end if
        Start Timeout1(READY_Send_Delay)
        Current_State = WAIT_SEND_READY
      else
        Current_State = WAIT_CONTINUE
      end if
    else
      Disable and reset local SUT-interface functions
      Auto_Continue = FALSE
      Start Timeout1(READY_Send_Delay)
      Current_State = WAIT_SEND_READY
    end if

  WAIT_SEND_READY:
    if (Operator_Input = STOP) or (Test_Controller_Message != no_message),
      Send STOP message
      Current_State = WAIT_CONTINUE
    elsif (Timeout1),
      Send READY message
      Start Timeout2(READY_Echo_Delay_Max)
      Current_State = WAIT_READY_ECHO
    else
      Current_State = DELAY_READY
    end if

  WAIT_READY_ECHO:
    if (Operator_Input = STOP) or
      ((Test_Controller_Message != no_message) and
      (Test_Controller_Message != READY)) or
      (Timeout2),
      Send STOP message
      Current_State = WAIT_CONTINUE

```

Figure 13: CCP Process for the PE Emulator and the Bus Monitor (continued)

```
elseif (Test_Controller_Message = READY),
    Current_State = WAIT_ROUND_INDEX
else
    Current_State = WAIT_READY_ECHO
end if

WAIT_ROUND_INDEX:
if (Operator_Input = STOP) or
    ((Test_Controller_Message != no_message) and
    (Test_Controller_Message != valid_round_index)) or
    (Timeout2),
    Send STOP message
    Current_State = WAIT_CONTINUE
elseif (Test_Controller_Message = valid_round_index),
    Set Round_Index = Test_Controller_Message
    Enable local SUT-interface functions
    Begin collection of SUT data records
    Current_State = WAIT_SUT_STATUS
else
    Current_State = WAIT_ROUND_INDEX
end if

WAIT_SUT_STATUS:
if (Operator_Input = STOP) or (Test_Controller_Message != no_message) or
    (SUT_Status = FAILED),
    End collection of SUT data records
    Send STOP message
    Current_State = SAVE_DATA_RECORDS
elseif (SUT_Status = TRUSTED),
    Send START message
    Start Timeout3(START_Echo_Delay_Max)
    Current_State = WAIT_START_ECHO
else
    Current_State = WAIT_SUT_STATUS
end if

WAIT_START_ECHO:
if (Operator_Input = STOP) or
    ((Test_Controller_Message != no_message) and
    (Test_Controller_Message != START)) or
    (SUT_Status != TRUSTED) or (Timeout3),
    End collection of SUT data records
    Send STOP message
    Current_State = SAVE_DATA_RECORDS
elseif (Test_Controller_Message = START),
    Discard accumulated SUT data records
    Start Timeout4(Round_Completion_Delay)
    Current_State = WAIT_ROUND_COMPLETION
else
    Current_State = WAIT_START_ECHO
```

Figure 13: CCP Process for the PE Emulator and the Bus Monitor (continued)

```
end if

WAIT_ROUND_COMPLETION:
  if (Operator_Input = STOP) or (Test_Controller_Message != no_message) or
    (SUT_Status = FAILED)
    End collection of SUT data records
    Send STOP message
    Current_State = SAVE_DATA_RECORDS
  elsif (Timeout4),
    Auto_Continue = TRUE
    End collection of SUT data records
    if (SUT data records show SUT-originated errors during round)
      Send STOP message
      Current_State = SAVE_DATA_RECORDS
    else
      Current_State = WAIT_ROUND_COMPLETION
    end if

SAVE_DATA_RECORDS:
  Save collected SUT data records to file (filename suffix: Round_Index)
  Transfer file to repository
  Current_State = WAIT_CONTINUE
```

7. Health Checks

Each hardware configuration HIRF test will be preceded and followed by a hardware configuration **Health Check** consisting of a two-hour run without radiation. A Health Check will also be performed after every change to the hardware components of the tested hardware configuration. The purpose of these checks is to confirm that the system is operating properly before a HIRF test and to expose any damage caused by the radiation. The health checks provide assurance that errors detected during a HIRF test are due to the effect of the field on the targeted components and not due to the monitoring system or SUT components outside the radiation chamber.

8. Shielding and Grounding

Figure 14 shows a RSPP node in its normal configuration when placed outside the test chamber. The enclosure is made of aluminum, and the endcaps are attached to the extrusion via metal screws. Power is delivered to the node by a shielded power cable grounded at the source end. The power cable shield is electrically attached to the connector at the node, thus grounding the enclosure. The optical fibers and the power cable are the only external connections.

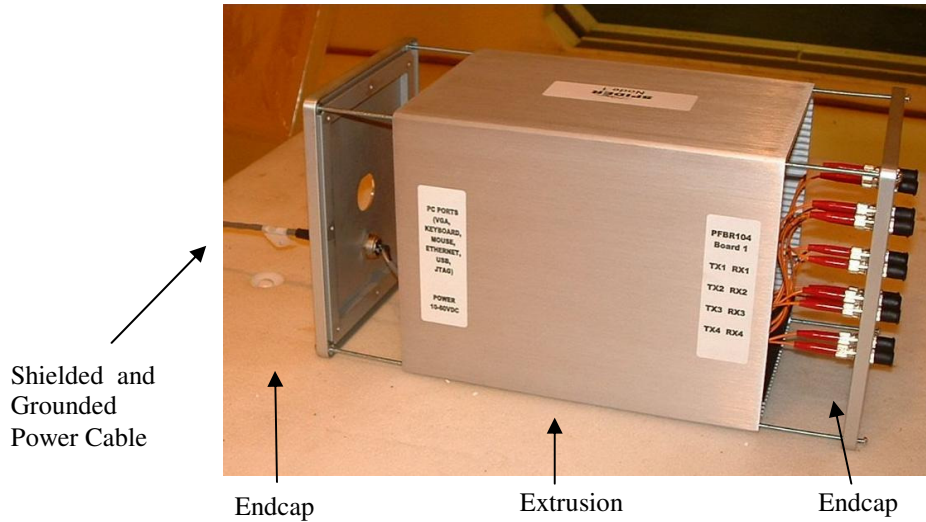


Figure 14: RSPP Node in Normal Configuration

Figure 15 shows a RSPP node in its configuration when it is inside the test chamber. All the targeted components will have the extrusions of the shielding enclosures removed in order to allow the electromagnetic field to directly reach the electronic components. In this configuration, only the endcap connected to the power cable is grounded.

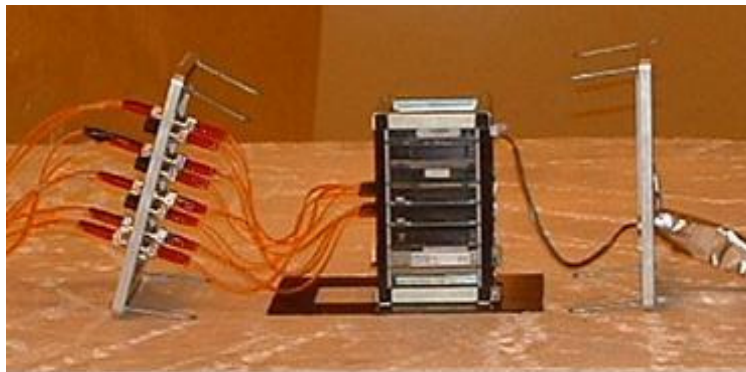


Figure 15: RSPP Node in Targeted Configuration Inside the Test Chamber

9. Equipment Layout

Figures 16 to 22 show the test setups for all the hardware configurations. The PE Emulator, Bus Monitor, and all the nodes inside the Control Room will receive 24V DC power from individual power supplies connected to standard AC wall outlets. The nodes inside Chamber A will receive 24V DC power from a power source controlled by the Test Controller. In order to minimize the distortion to the field characteristics experienced by the nodes inside Chamber A, the nodes will be separated from each other, from the chamber walls, floor and ceiling, and from any other metallic objects by at least 1.5 m (i.e., one

half wavelength at the lowest test frequency). The targeted nodes inside Chamber A will be placed on top of foam blocks or tables to provide support and ensure separation from the chamber floor.

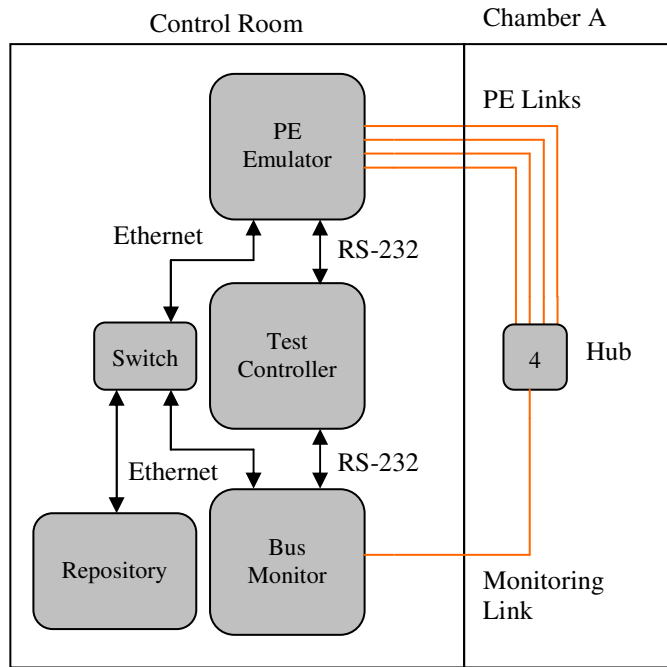


Figure 16: Test Setup for Hardware Configurations HC1 and HC2

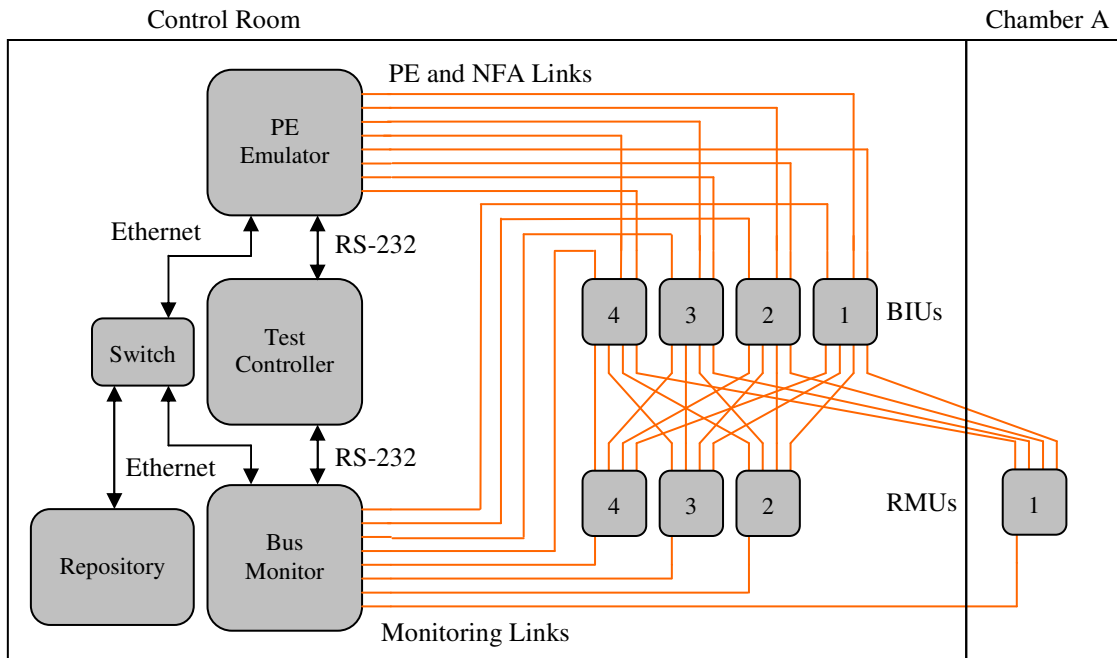


Figure 17: Test Setup for Hardware Configurations HC3 and HC6

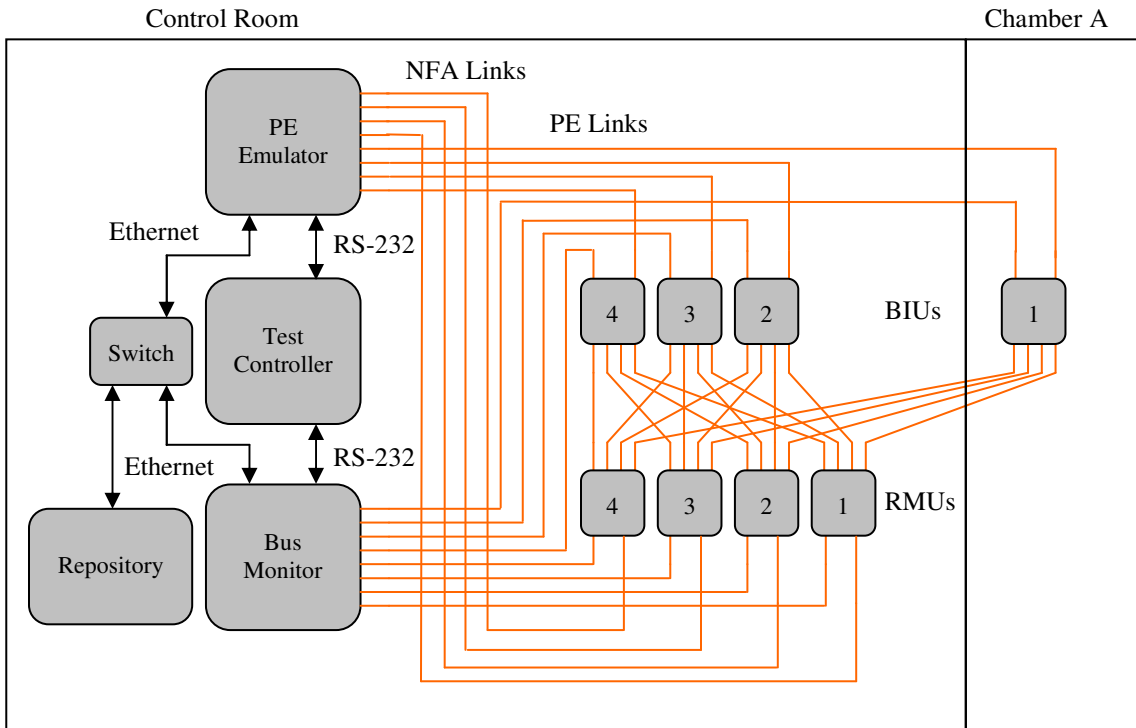


Figure 18: Test Setup for Hardware Configurations HC4 and HC7

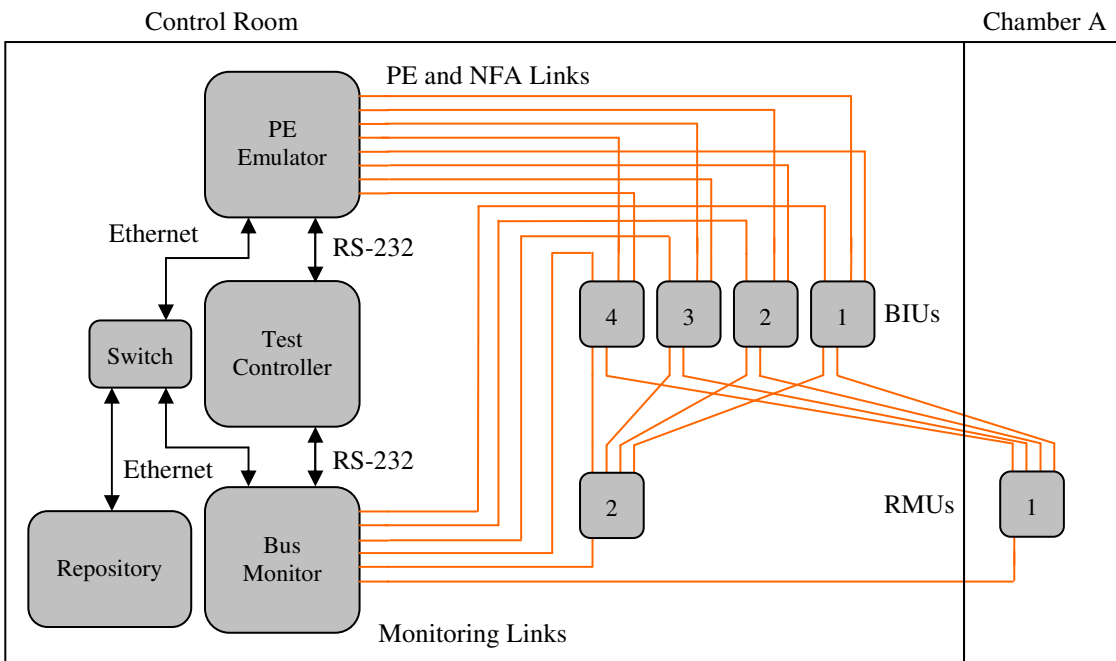


Figure 19: Test Setup for Hardware Configurations HC5 and HC8

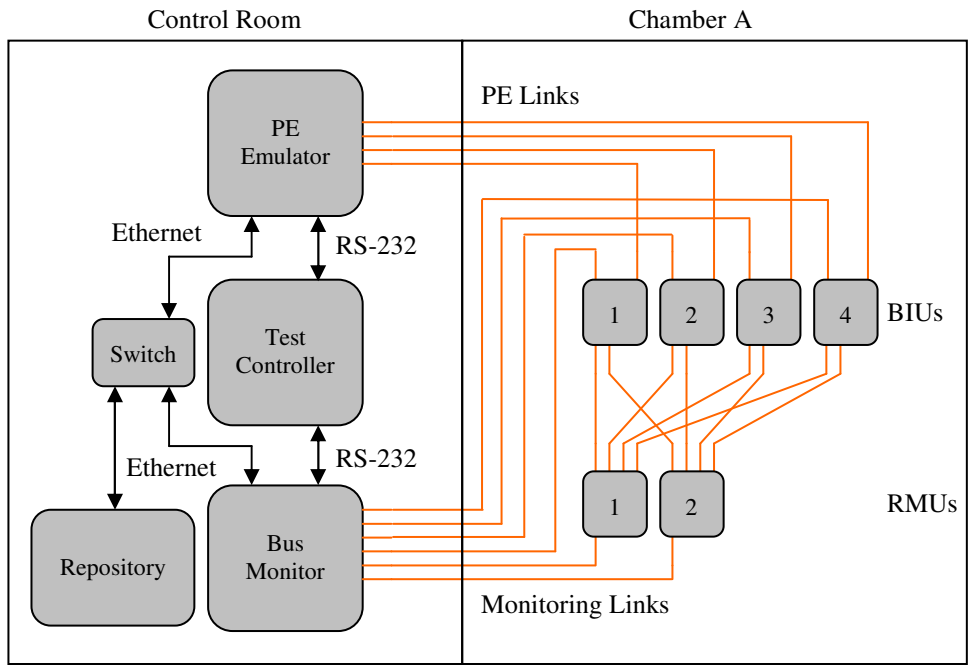


Figure 20: Test Setup for Hardware Configurations HC9 and HC12

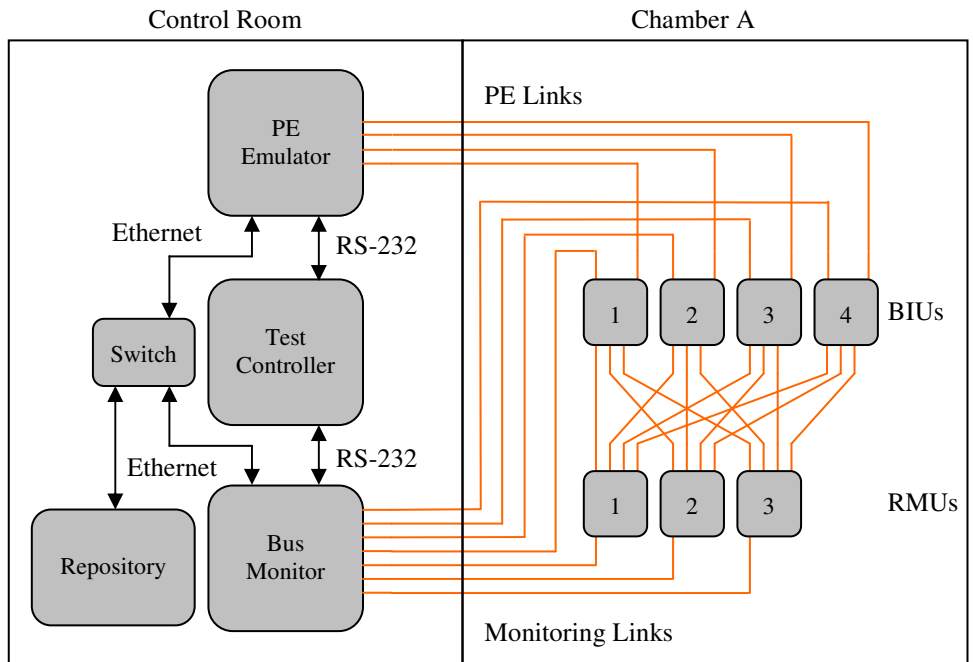


Figure 21: Test Setup for Hardware Configurations HC10 and HC13

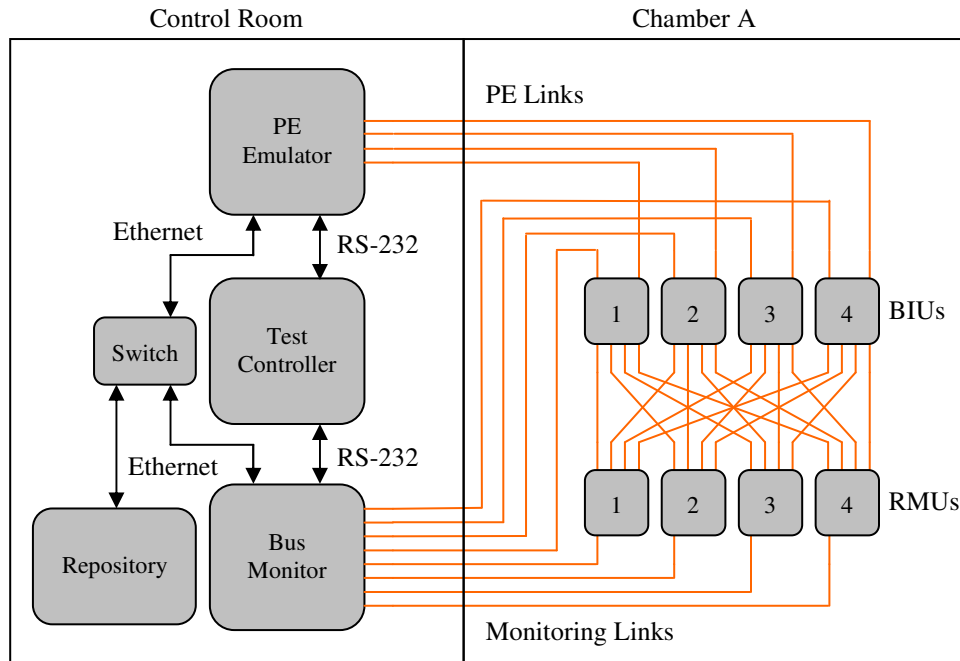


Figure 22: Test Setup for Hardware Configurations HC11 and HC14

References

- [1] Fuller, Gerald L.: *Understanding HIRF – High Intensity Radiated Fields*. Aviation Communications, Inc., Leesburg, VA, 1995, p. 7-2.
- [2] Hess, Richard: *Computing Platform Architectures for Robust Operation in the Presence of Lightning and Other Electromagnetic Threats*. Presented at the 16th Digital Avionics Systems Conference (DASC), Irvine, California, October 26-30, 1997
- [3] Miner, Paul S.; Malekpour, Mahyar; and Torres, Wilfredo: *A Conceptual Design for a Reliable Optical Bus (ROBUS)*. Presented at the 21st Digital Avionics Systems Conference (DASC), Irvine, California, October 27-31, 2002.
- [4] Torres-Pomales, Wilfredo; Malekpour, Mahyar; and Miner, Paul S.: *ROBUS-2: A Fault-Tolerant Broadcast Communication System*. NASA TM-2005-213540, 2005.
- [5] Torres-Pomales, Wilfredo; Malekpour, Mahyar; and Miner, Paul S.: *Design of the Protocol Processor for the ROBUS-2 Communication System*. NASA TM-2005-213934, 2005.
- [6] RTCA DO-160D, Change No. 1, “Environmental Conditions and Test Procedures for Airborne Equipment”, Section 20, “Radio Frequency Susceptibility (Radiated and Conducted)”, December 2000.
- [7] Ladbury, J.; Koepke, G.; Camell, D.: “Evaluation of the NASA Langley Research Center Mode-Stirred Chamber Facility”, NIST Technical Note 1508, January 1999.
- [8] <http://opensource.arc.nasa.gov/project/robus-2/>

Acronyms

ASCII	American Standard Code for Information Interchange
BIU	Bus Interface Unit
CCP	Controller Coordination Protocol
COTS	Commercial Off-The-Shelf
CPU	Central Processing Unit
CW	Continuous Wave
DC	Direct Current
DSI	Derivation Systems, Inc.
EM	Electromagnetic
EMI	Electromagnetic Interference
FHSTC	Fine HIRF Susceptibility Threshold Characterization
FPGA	Field Programmable Gate Array
FSM	Finite State Machine
HC	Hardware Configuration
HEC	HIRF Effects Characterization
HFA	Hub Fault Analyzer
HIRF	High Intensity Radiated Field
HSTC	HIRF Susceptibility Threshold Characterization
IVHM	Integrated Vehicle Health Management
LUF	Lowest Usable Frequency
Mbps	Mega-bits per second
NFA	Node Fault Analyzer
NIST	National Institute of Standards and Technology
PE	Processing Element
RC	Reverberation Chamber
RF	Radio Frequency
RMU	Redundancy Management Unit
ROBUS	Reliable Optical Bus
RPP	ROBUS Protocol Processor
RSPP	Reconfigurable SPIDER Prototyping Platform
RTCA	Radio Technical Commission for Aeronautics
SBIR	Small Business Innovation Research
SHM	System Health Monitor
SPIDER	Scalable Processor-Independent Design for Extended Reliability
SUT	System Under Test
TCS	Test Control System
TDMA	Time Division Multiple Access

REPORT DOCUMENTATION PAGE

*Form Approved
OMB No. 0704-0188*

The public reporting burden for this collection of information is estimated to average 1 hour per response, including the time for reviewing instructions, searching existing data sources, gathering and maintaining the data needed, and completing and reviewing the collection of information. Send comments regarding this burden estimate or any other aspect of this collection of information, including suggestions for reducing this burden, to Department of Defense, Washington Headquarters Services, Directorate for Information Operations and Reports (0704-0188), 1215 Jefferson Davis Highway, Suite 1204, Arlington, VA 22202-4302. Respondents should be aware that notwithstanding any other provision of law, no person shall be subject to any penalty for failing to comply with a collection of information if it does not display a currently valid OMB control number.
PLEASE DO NOT RETURN YOUR FORM TO THE ABOVE ADDRESS.

1. REPORT DATE (DD-MM-YYYY) 01-05 - 2008			2. REPORT TYPE Technical Memorandum		3. DATES COVERED (From - To)	
4. TITLE AND SUBTITLE Plan for the Characterization of HIRF Effects on a Fault-Tolerant Computer Communication System					5a. CONTRACT NUMBER	
					5b. GRANT NUMBER	
					5c. PROGRAM ELEMENT NUMBER	
6. AUTHOR(S) Torres-Pomales, Wilfredo; Malekpour, M. R.; Miner, Paul S.; and Koppen, Sandra V.					5d. PROJECT NUMBER	
					5e. TASK NUMBER	
					5f. WORK UNIT NUMBER 645846.02.07.07.07	
7. PERFORMING ORGANIZATION NAME(S) AND ADDRESS(ES) NASA Langley Research Center Hampton, VA 23681-2199					8. PERFORMING ORGANIZATION REPORT NUMBER L-19453	
9. SPONSORING/MONITORING AGENCY NAME(S) AND ADDRESS(ES) National Aeronautics and Space Administration Washington, DC 20546-0001					10. SPONSOR/MONITOR'S ACRONYM(S) NASA	
					11. SPONSOR/MONITOR'S REPORT NUMBER(S) NASA/TM-2008-215306	
12. DISTRIBUTION/AVAILABILITY STATEMENT Unclassified - Unlimited Subject Category 62 Availability: NASA CASI (301) 621-0390						
13. SUPPLEMENTARY NOTES An electronic version can be found at http://ntrs.nasa.gov						
14. ABSTRACT This report presents the plan for the characterization of the effects of high intensity radiated fields on a prototype implementation of a fault-tolerant data communication system. Various configurations of the communication system will be tested. The prototype system is implemented using off-the-shelf devices. The system will be tested in a closed-loop configuration with extensive real-time monitoring. This test is intended to generate data suitable for the design of avionics health management systems, as well as redundancy management mechanisms and policies for robust distributed processing architectures.						
15. SUBJECT TERMS HIRF; Avionics data bus; Distributed processing; Fault tolerance; Redundancy management; Test automation						
16. SECURITY CLASSIFICATION OF:			17. LIMITATION OF ABSTRACT	18. NUMBER OF PAGES	19a. NAME OF RESPONSIBLE PERSON	
a. REPORT	b. ABSTRACT	c. THIS PAGE			STI Help Desk (email: help@sti.nasa.gov)	
U	U	U	UU	43	19b. TELEPHONE NUMBER (Include area code) (301) 621-0390	